

Analysis of SAC-OCDMA system to reduce MAI using Fiber Bragg Gratings and MDW codes

RAKESH GOYAL^{*}, NAVPREET KAUR, RAJINDER SINGH KALER^a, MONIKA RANI^b

D.A.V. University, Jalandhar, Punjab, India

^aThapar University, Patiala, Punjab, India

^bPCM S. D. College for Women, Jalandhar, Punjab, India

In this manuscript, we have analyzed a Spectral Amplitude Coding-Optical Code Division Multiple Access (SAC-OCDMA) System. The uniform Fiber Bragg Gratings (FBGs) are used at transmitter and receiver end to improve the overall performance of the system. Multiple Access Interference (MAI) has been reduced using a mathematical model and MDW codes for the proposed system. Further, we have transmitted data at 100 Gbps rate up to a distance of 80 Km by increasing the ten numbers of FBGs. The proposed system has been analyzed in terms of output power, distance, BER and Quality Factor. The Optisystem7 tool has been used to analyze the system performance.

(Received September 20, 2015; accepted August 3, 2016)

Keywords: OCDMA, FBG, MAI, MDW, SAC

1. Introduction

Code Division Multiple Access (CDMA) has been well studied in the wireless communication systems. Recently, the spread spectrum technique has gotten a lot of attention in the optical fiber transmission due to the inherent large bandwidth of fibers. OCDMA has several benefits such as asynchronous transmission, flexibility in network design, accommodation of burst traffic and variable bit rate traffic [1]. Nevertheless, the OCDMA systems suffer from certain noises such as PIIN, shot noise and thermal noise etc. In these networks, Multiple Access Interference (MAI) is the main factor responsible for performance degradation, especially, when a large number of users are involved in the OCDMA systems. Therefore, the most important consideration is the code designs for reducing contribution of the MAI at the optical power receiver end. Among all OCDMA techniques, Spectral Amplitude Coding (SAC) has the advantages of suppressing the effect of MAI due to its flexibility in phase cross-correlation which can be utilized as address sequence and balance detection at the receiver side [2]. In this manuscript, we have analyzed the OCDMA system based on FBG through the mathematical model and exhaustive optical simulator called Optisystem7 software from Optiwave.

2. Theory

A. OCDMA: The aim of OCDMA is to take benefits of radio frequency communications with sharing of the huge optical bandwidth. The block diagram for OCDMA is shown in Fig. 1.

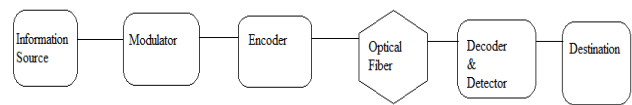


Fig. 1. Block Diagram of OCDMA

An OCDMA system for each user can be described by a data source, containing the data that will be sent, followed by an encoder and then a laser which maps the signal from electrical form to an optical pulse sequence. At the receiver end, an optical correlator is used to extract the encoded data. Many subscribers transmit data simultaneously [3]. Each user has its own codeword, which is approximately orthogonal to all other code words. The encoded data is sent to the Nx1 star coupler, from where the optical channel carries the signal through the optical fiber and couples to a 1xN coupler and broadcast to all nodes [4]. All users encoded data are then added together chip by chip and the result, which is called the superposition, are sent over the channel. The individual receivers consisting of optical correlate continuously observe the superposition of all incoming pulse transmission and recover the data from the corresponding transmitter. This is done by correlation between the incoming signal and stored copies of that user unique sequence [5].

B. FIBER BRAGG GRATING: A fiber bragg grating (FBG) is a type of distributed bragg reflector constructed in a short segment of optical fiber that reflects particular wavelengths of light and transmits all others. This is achieved by creating a periodic variation in there refractive index of the fiber core, which

generates a wavelength-specific dielectric mirror. A fiber Bragg grating can therefore be used as an inline optical filter to block certain wavelengths, or as a wavelength-specific reflector. The advantages of FBGs in systems applications include low insertion loss, all fiber compatibility, relative ease of manufacture and low cost; but a major feature is that by changing the grating parameters such as induced index change, length, period chirp, fringe tilt, we can achieve the desired grating spectral characteristics [6].

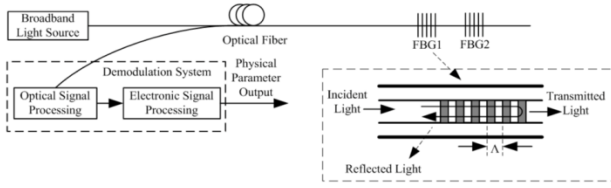


Fig. 2. Block diagram of a Fiber Bragg Grating [6]

The fundamental principle behind the operation of a FBG is reflection, where light travelling between media of different refractive indices may both reflect and refract at the interface. The refractive index will typically alternate over a defined length. The reflected wavelength (λ_B), called the Bragg wavelength, is defined by the relationship [6]

$$\lambda_B = 2n_e\Lambda \quad (1)$$

Where n_e is the effective refractive index of the grating in the fiber and Λ is the grating period. The effective refractive index quantifies the velocity of propagating light as compared to its velocity in vacuum. n_e Depends not only on the wavelength but also (for multimode waveguides) on the mode in which the light propagates. For this reason, it is also called modal index [7].

The wavelength spacing ($\Delta\lambda$) is (in the strong grating limit) given by [7]

$$\Delta\lambda = \left[\frac{2\delta n_0 \eta}{\pi} \right] \lambda_B \quad (2)$$

Where δn_0 is the variation in the refractive index ($n_3 - n_2$), and η is the fraction of power in the core. Note that this approximation does not apply to weak gratings where the grating length (L_g) is not large compared to $\lambda_B / \delta n_0$.

The peak reflection ($P_B(\lambda_B)$) is approximately given by,

$$P_B(\lambda_B) \approx \tanh^2 \left[\frac{N\eta(V)\delta n_0}{n} \right] \quad (3)$$

Where N is the number of periodic variations, the full equation for the reflected power ($P_B(\lambda)$), is given by [7],

$$P_B(\lambda) = \frac{\sinh^2 \left[\eta(V)\delta n_0 \sqrt{1 - \Gamma^2 \frac{N\Lambda}{\lambda}} \right]}{\cosh^2 \left[\eta(V)\delta n_0 \sqrt{1 - \Gamma^2 \frac{N\Lambda}{\lambda}} \right] - \Gamma^2} \quad (4)$$

C. MODIFIED DOUBLE WEIGHT (MDW)

CODE: The code structure is based on Modified Double Weight (MDW) code families for SAC-OCDMA systems. The MDW codes have a large number of weight which can be developed through double weight (DW) code of weight two, the MDW code is the modified version of DW code. The MDW code possesses ideal cross-correlation properties and exists for every natural number. However, the MDW code weight can be any even number that is greater than 2. Moreover, the MDW codes can also be represented by using the ($K \times N$) matrix. The details of code structure and code parameters have been presented in [8].

$$\begin{bmatrix} 0 & 0 & 00 & 1 & 10 & 11 \\ 0 & 1 & 10 & 0 & 01 & 10 \\ 1 & 0 & 01 & 1 & 01 & 00 \end{bmatrix} \quad (5)$$

We can increase the number of users from 1 to 3 while the weight is still fixed at 4. An MDW code with weight of 4 denoted by ($N, 4, 1$) for any given code length N , can be related to the number of users K through [9]:

$$N = 3K + \frac{3}{8} \left[\sin\left(\frac{k\pi}{3}\right) \right]^2 \quad (6)$$

Let $C(i)K$ denote the i th element of the K th MDW code sequences, and according to the properties of MDW code, the direct detection technique can be written as

$$\sum_{i=1}^N C_k(i)C_l(i) = \begin{cases} W & \text{for } k = l \\ 1 & \text{else} \end{cases} \quad (7)$$

3. Results and discussion

The simulation setup for OCDMA shown in Fig. 3 by constructing a matched decoder pair from the MDW code set. We have utilized the advantages of distinct frequency chips and small available tunable window and then SAC technique is employed over each slot using a coder based upon MDW codes and ultra-high resolution optical demultiplexer [10]. Optical attenuator and a logical fork to split the signal having the physical parameters like Bessel's transfer function and stop bandwidth is equivalent to eight times the bit rate. It can be shown that this encoder encodes the data both in wavelength and in time domain [11, 12].

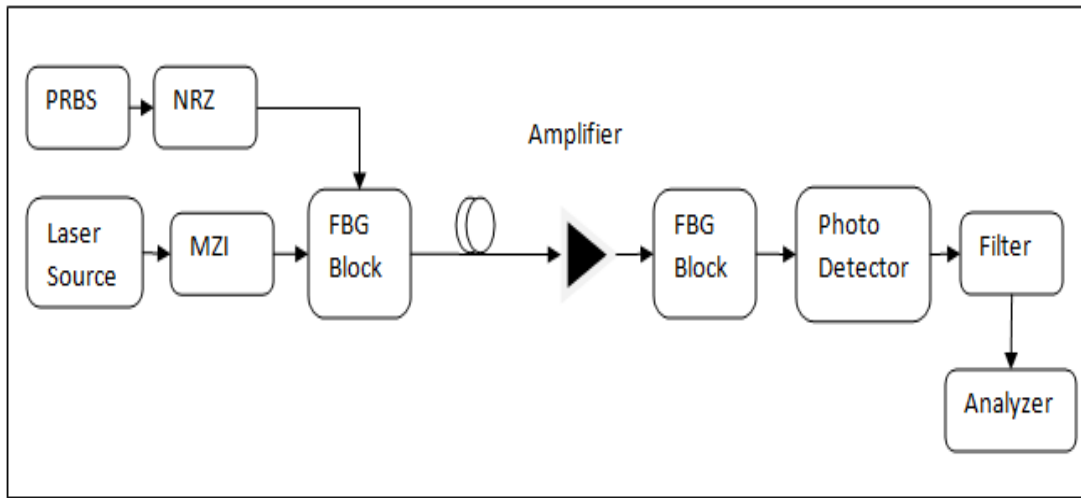


Fig. 3. Proposed Architecture of SACOCDMA with MDW Code

In the simulation, uniform FBGs are used to implement the MDW code by spectral amplitude encoding. The signal is generated using an incoherent source modulated with NRZ and PRBS data using a Mach-Zehnder Modulator. The optical link is of varying length of single mode fiber. The receiver is comprised of a spectral filter and a photo detector connected in a balanced configuration which performs the decoding with a low-pass filter and BER analyzer. In the results, the whole simulation is compared on comparisons of Different FBG.

Table 3. BER and Q factor for 100 Gbps data rate at different fiber lengths

Length of fiber	BER on FBG	Q factor
30 km	2.54*e-070	17.67
60 km	8.92*e-034	12.7878
90 km	4.78*e-014	7.4434
120 km	3.45*e-005	3.9769
150 km	0.008468	2.38786
180 km	0.015286	2.50199

Table 1. BER and Q factor for 40Gbps data rate at different fiber lengths

Length of fiber	BER on FBG	Q factor
30 km	1.65*e-249	33.71
60 km	9.85*e-031	11.4651
90 km	2.35*e-005	4.06842
120 km	0.00025	3.468
150 km	0.004389	2.99151
180 km	0.00138	2.6199

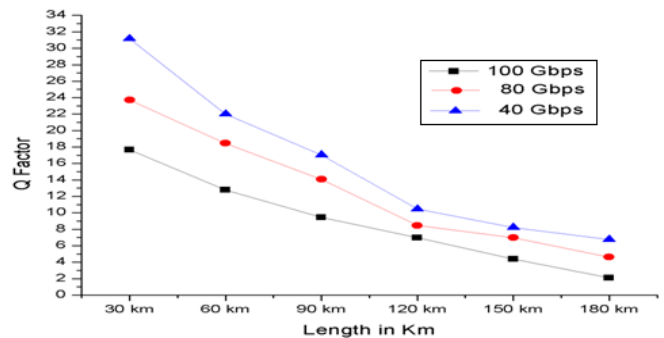


Fig. 4. Q factor Vs distance at different data rates

Table 2. BER and Q factor for 80 Gbps data rate at different fiber lengths

Length of fiber	BER on FBG	Q factor
30 km	0	41.17
60 km	1.58*e-033	12.009
90 km	2.24*e-007	5.04595
120 km	4.00*e-006	4.4588
150 km	1.20*e-005	4.22098
180 km	7.92*e-005	3.76628

A comparison between the SAC OCDMA at different data rates i.e. 40 Gbps, 80Gbps and 100 Gbps is given in Fig. 4. We can observe that at 40 Gbps for the conventional system gives better results than the others and it also degrades with the increase in distance. The reason behind this is as follows; for small distance the beat noise is negligible and thermal noise and shot noise are the main limiting factors. The very low BER (below 10 and 15) is due to the small data rate where the beat noise effect is negligible especially in the controlled multi laser source configuration. Fig. 5 shows the BER versus the distance at data rate 40Gbps, 80 Gbps and 100 Gbps. On the other

hand, faulty transmission is obtained for all data rates for the system. It is important to note that for this system to support higher data rate the bin spectral bandwidth must be increased. This will lead to an increase in the spacing between the adjacent lasers, which will decrease the beat noise and thus increase the data rate.

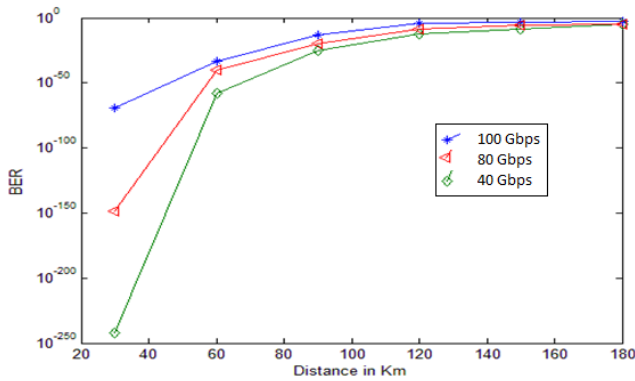


Fig. 5. BER Vs Distance

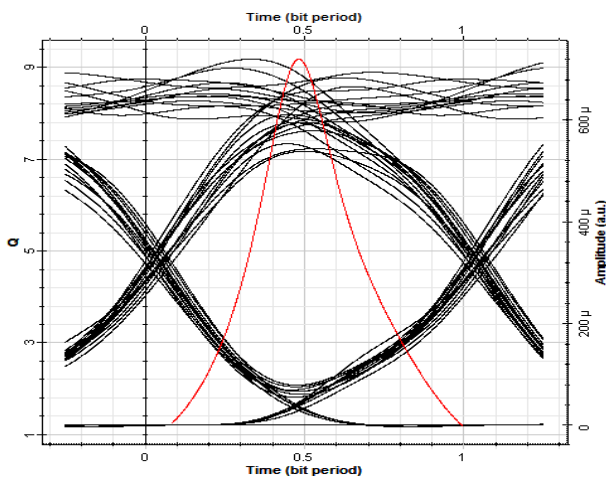


Fig. 6. Eye Diagram shows at 40 Gbps

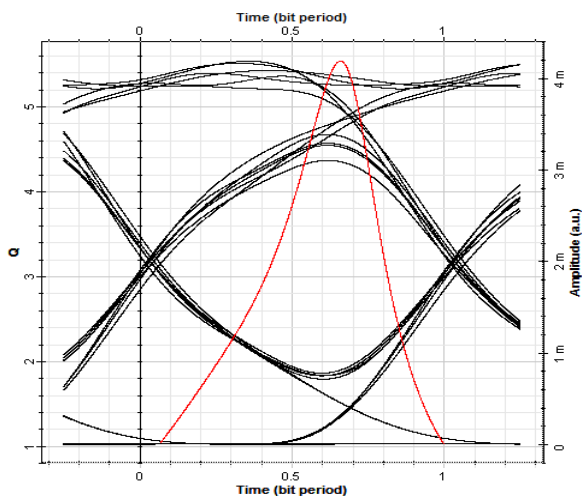


Fig. 7. Eye Diagram shows at 80 Gbps

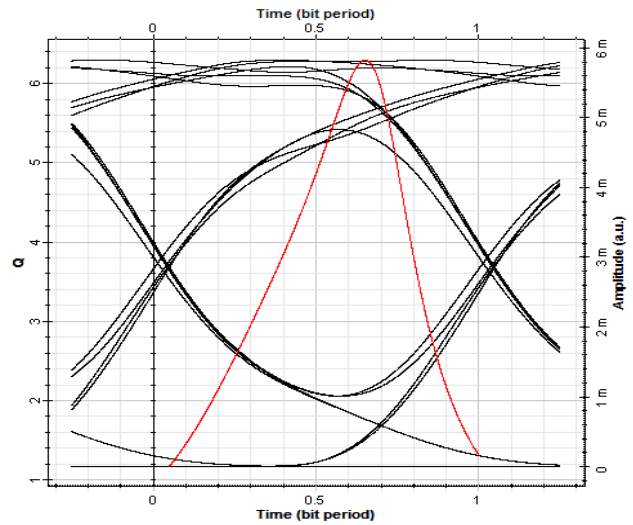


Fig. 8. Eye Diagram shows at 100 Gbps

The eye pattern diagrams for MDW code at different data rates like 40, 80,100Gbps at 80 km are shown in Fig. 6 to Fig. 8. The eyes diagram shown in Fig. 6 clearly depicts that the data rate at 40 Gbps gives better performance, having a larger eye opening than others. The vertical distance between the top of the eye opening and maximum signal level gives the degree of distortion.

4. Conclusion

In this paper, the analysis performance of OCDMA is presented with FBGs. To improve the BER of the system, the uniform FBG are used at the transmitter and receiver end. We have achieved 100 Gbps data rate transmission using the proposed network. The comparison of various data rates at different fiber lengths has been shown. The higher BER 1.6587×10^{-245} is considered at distance 30 Km. By using 10 FBGs the length of the fiber can be increased up to 180 Km distance with minimum acceptable BER.

References

- [1] A. M. Alhassan, N. M. Saad, N. Badruddin, IEEE Photonics Technology Letters **23**(13), 875 (2011).
- [2] S. Abd El Mottaleb, H. A. Fayed, A. A. E. Aziz, A. M. H., IOSR Journal of Electronics and Communication Engineering **9**(2), 55 (2014).
- [3] H. M. R. Al- Khafaji, S. A. Aljunid, H. A. Fadhil, International Journal of Computer and Electrical Engineering **4**(6), 861 (2012).
- [4] I. F. Radhi, T. H. Abd, S. A. Aljunid, H. A. Fadhil, Journal of Applied Science Research **8**(1), 331 (2012).
- [5] H. A. Fadhil, S. A. Aljunid, R. Badlishah, F. N. Hasoon, M. S. Anuar, International Journal of Computer Science and Network Security **7**(11), 258 (2007).

-
- [6] J. Chen, B. Liu, H. Zhang, *Optoelectronics China* **4**(2), 204 (2011).
- [7] E. Guide, An educational resource published by *Communication* **8**, (2009).
- [8] S. G. Abdulqader, S. A. Aljunid, H. M. R. Al-Khafaji, H. A. Fadhil, *Journal of Communications* **9**(2), 99 (2014).
- [9] H. M. R. Al- Khafaji, S. A. Aljunid, A. Amphawan, H. A. Fadhil, *IEEE Symposium on industrial Electronics And Applications* **7**(1), 44 (2013).
- [10] S. G. Abdulqader, H. A. Fadhil, S. A. Aljunid, *Journal of Theoretical and Applied Information technology* **67**(2), 368 (2014).
- [11] R. K. Zakiah Sahbudin, M. Kamaruizaman, S. Hitam, M. Mokhtar, S. B. Ahmad Anas, *Optik- int. j. light* **10**(10), 1 (2012).
- [12] M. K. Abdullah, F. N. Hasoon, S. A. Aljunid, S. Shaari, *Optics Communications* **281**(1), 4658 (2008).

*Corresponding author: er.rakeshgoyal@gmail.com